ACS APPLIED MATERIALS & INTERFACES

Research Article

www.acsami.org

Interfacial Properties of Lignin-Based Electrospun Nanofibers and Films Reinforced with Cellulose Nanocrystals

Mariko Ago,*[,†,‡] Joseph E. Jakes,[§] Leena-Sisko Johansson,[⊥] Sunkyu Park,[†] and Orlando J. Rojas*[,†,⊥]

[†]North Carolina State University, Departments of Forest Biomaterials and Chemical and Biomolecular Engineering, Raleigh, North Carolina 27695, United States

[‡]Tokushima Bunri University, Faculty of Science and Engineering, Sanuki, Kagawa, Japan

[§]Performance Enhanced Biopolymers, USDA Forest Service, Forest Products Laboratory, Madison, Wisconsin 53726, United States

[⊥]Aalto University, School of Chemical Technology, Department of Forest Products Technology, FI-00076 Aalto, Espoo, Finland

Supporting Information

ABSTRACT: Sub-100 nm resolution local thermal analysis, X-ray photoelectron spectroscopy (XPS), and water contact angle (WCA) measurements were used to relate surface polymer distribution with the composition of electrospun fiber mats and spin coated films obtained from aqueous dispersions of lignin, polyvinyl alcohol (PVA), and cellulose nanocrystal (CNC). Defect-free lignin/PVA fibers were produced with radii which were observed to increase with lignin concentration and with the addition of CNCs. XPS and WCA results indicate a nonlinear relationship between the surface and the bulk compositions. A threshold around 50 wt % bulk composition was identified in which extensive partitioning of PVA and lignin components occurred on the surface below and above this value. In 75:25 wt % lignin/PVA solvent cast films, phase separated domains were observed. Using nanoscale thermal analyses, the continuous phase was determined to be lignin-rich and the discontinuous phase had a lignin/PVA dispersion. Importantly, the size of the phase separated domains was reduced by the addition of CNCs. When electrospun fiber surfaces were lignin-rich, the addition of CNCs affected their surfaces. In contrast, no surface effects were observed with the addition of CNCs in PVA-rich fibers. Overall, we highlight the importance of molecular interactions and phase separation on the surface properties of fibers from lignin as an abundant raw material for the fabrication of new functional materials.

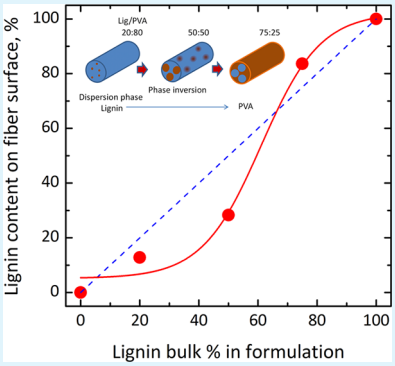

KEYWORDS: *lignin, films, fibers, electrospinning, cellulose nanocrystals, contact angle, X-ray photoelectron spectroscopy, space-resolved AFM-thermal transitions*

INTRODUCTION

Electrospinning is ideal for the production of random fiber mats that are flexible and porous. Because the mats have nano- to micrometer features, they have high surface area to volume ratios and can display unique mechanical, thermal, and catalytic properties compared to what they exhibit on a macroscale.[1−3] Electrospun fiber mats are suitable for designing novel materials and components in a variety of applications, including filters, sensors, medical textiles, and flexible coatings.[4−8] Many polymer systems have been used to electrospin fibers;[2,9,10] however, in this work, we focus on lignin-based systems. Lignin is an attractive material because it is readily available as a byproduct from biomass processing, biorefineries, and second generation bioethanol operations.[11] Applications for lignin already investigated include precursors for carbon fiber,[12,13] engineering plastics,[14−18] and adsorbents and adhesive materials.[19−22] Recently, we reported novel nanofiber systems produced by electrospinning aqueous dispersions of lignin, polyvinyl alcohol (PVA), and cellulose nanocrystals (CNCs). We correlated the properties of the starting aqueous dispersion (viscosity, electro-conductivity, and surface tension) with electrospinnability.[23] Also, the mats were observed to have excellent thermal properties that were mainly ascribed to the strong intermolecular hydrogen bonding between hydroxyl groups of the lignin/PVA matrix and the dispersed CNCs.

In this study, we investigate the morphology of the lignin/PVA/CNC electrospun fibers with emphasis on understanding the distribution of polymers on the fiber surfaces as related to the fiber composition. An understanding of fiber surface properties, such as surface energy, is needed to tailor electrospun mats for different applications, including tissue engineering, drug delivery, membranes, fuel cells, and aerospace materials. The morphology of electrospun lignin-based fibers and respective reference films are investigated here using sub-100 nm local thermal analysis, X-ray photoelectron spectroscopy (XPS), and water contact angle (WCA) measurements.

Received: September 16, 2012
Accepted: November 27, 2012
Published: November 27, 2012

EXPERIMENTAL SECTION

Lignin/PVA solutions and lignin/PVA/CNC dispersions were prepared according to the method described previously.[23] Lignin (kraft lignin from softwood) was obtained from Sigma-Aldrich (St. Louis, MO) with reported molecular weight of 10 kDa (alkali lignin, low sulfur, CAS Number: 8068-05-1). The lignin was used as received. Poly(vinyl alcohol) (PVA) was acquired from the same supplier under trade name Mowiol 20-98 (CAS Number: 9002-89-5), with reported molecular weight of 125 kDa and degree of hydrolysis of 98% (2% acetyl groups).

Cellulose nanocrystals (CNCs) were prepared by acid hydrolysis of pure cotton. Cotton was first acid hydrolyzed with 65 wt % sulfuric acid at 50 °C for 20 min. The resulting dispersion was poured into ~500 g of ice cubes and washed with distilled water until obtaining neutral pH by successive centrifugation at 12 000 rpm (10 °C, 20 min). Dialysis for 1 week against deionized water with 12 000 MWCO membranes (Spectrum Laboratories, Inc., USA) was performed to remove trace amounts of residual sulfuric acid from the suspension. The dimensions of the obtained CNCs (Figure S1 of Supporting Information) were typically 100−150 nm in length and 10−20 nm in width, in agreement with values reported elsewhere.[24,25] The obtained CNC dispersion was sonicated for 15 min with a probe-type sonicator operated at 250 W to avoid nanoparticle aggregation and kept refrigerated at 4 °C until use. The concentration of CNCs in the dispersions was determined gravimetrically.

Multicomponent Electrospun Fibers, Spin Coated and Solvent Casted Films. Aqueous PVA solutions (5 or 8 wt % concentration) were prepared, and lignin was added to obtain solutions with lignin/PVA dry mass ratios of 0:100, 20:80, 50:50, and 75:25. Aqueous dispersions of 4.5 wt % CNCs were added to the lignin/PVA 20:80 and 75:25 solutions to obtain dispersions with 5, 10, and 15 wt % of CNCs based on dry mass. The dispersions were kept under vigorous mechanical agitation at 60 °C for 15 min, followed by cooling to room temperature under stirring for 120 min. Dispersions with less than one week storage time were used to produce the electrospun fibers, spin coated films, and solvent cast films.

For electrospinning, the suspensions were loaded into a 10 mL plastic, disposable syringe with a 22 gauge needle. The needle was connected to the positive terminal of a voltage generator designed to produce a voltage up to 50 kV DC (Glassman High Voltage, Series EL). A thin aluminum foil covering a 15 cm diameter aluminum plate was used as a collector. The plate was connected to the negative electrode of the power supply (ground) and set at a working distance of 22 cm. An operating voltage of 19 kV was used. A constant 8 μL/min flow rate was maintained during electrospinning using a computer-controlled syringe pump. Electrospinning was performed at room temperature and at 35−45% relative humidity. The collected electrospun mats were kept in a desiccator containing anhydrous $CaSO_4$.

Spin-coated films of lignin, PVA, and 75:25 lignin/PVA with and without CNCs were manufactured on top of silicon wafers. Silicon wafers (10 × 10 mm^2) were first cleaned thoroughly by immersion in 10 wt % NaOH solution, rinsed with distilled water and ethanol, and finally subjected to UV−ozone treatment. The lignin, PVA, and lignin/PVA solutions were spin coated onto the silicon surfaces by first using 2000 rpm for 2.5 min followed by 700 rpm for 30 s. In the case of lignin/PVA/CNC dispersions, the second spinning stage was conducted at 1500 rpm for 15 s. The films were dried at room temperature for 8 h followed by vacuum drying at 40 °C for 12 h (see Figure S2 of Supporting Information for atomic force microscopy images of spin-coated film surfaces).

Additionally, solid films were obtained by solvent casting 20:80 and 75:25 lignin/PVA solutions as well as 75:25/5% and 75:25/15% lignin/PVA/CNC dispersions. The film casting was carried out by pouring the solution onto a clean Teflon plate and storing them in a dust-free atmosphere overnight at room temperature to dry. The resulting films were between 20 and 100 μm thick detected by optical microscopy.

Fiber Characterization. The morphology of nanofibers in electrospun mats was examined using a field emission scanning electron microscope (FE-SEM, JEOL, 6400F) operating at 5 kV and a working distance of 11 mm. A small piece of the nanofiber mat was fixed on carbon tape and then sputtered with Au/Pt to obtain a coating layer thickness of about 4 nm. The diameter distribution was obtained from 40 fibers that were selected randomly and image-analyzed (Revolution software). Lignin/PVA electrospun fibers loaded with 15 wt % CNC (75:25/15%) were also imaged with a field emission in-lens scanning electron microscopy (FEI-SEM, Hitachi SU9000) operating at 1 kV and working distance of 2.6 mm.

Water Contact Angle. The contact angles of water droplets (4 μL volume) delivered from a needle connected to a syringe pump and deposited on the surface of electrospun mats and spin-coated films were measured with a Phoenix 300 system (SEO Corp., Korea). The images of the sessile drop were analyzed with respect to their width and height to yield the contact angle and drop volume using the "Image J" software (National Institutes of Health, U.S.). The averages of at least three contact angles for each substrate are reported.

X-ray Photoelectron Spectroscopy (XPS). The surface chemical composition of 20:80, 50:50, and 75:25 lignin/PVA electrospun fiber mats and lignin and PVA spin-coated films was determined using X-ray photoelectron spectroscopy (XPS). Electrospun fiber mats with thicknesses of ca. 100 μm were used in these measurements. The measurements were performed with an AXIS 165 (Kratos Analytical, Manchester, UK) spectrometer using a monochromated Al Kα X-ray source at 100 W. All samples were pre-evacuated overnight to stabilize ultrahigh vacuum (UHV) conditions. Each sample was analyzed at least on three different locations, together with ash-free 100% cellulose filter paper used in situ as a reference.[26] Elemental surface composition was determined from low resolution scans recorded with 80 eV pass energy and 1 eV steps. The carbon C 1s high resolution spectrum was collected using 20 eV pass energy at 0.1 eV steps. In XPS analysis, binding energies were charge-corrected in all high-resolution data using the aliphatic CC-carbon component at 285.0 eV.[27] XPS signals between 288 and 290 eV were identified and ascribed to contamination from the atmosphere and from sample handling. However, the binding energy region of these peaks did not interfere with the analyses that used the fingerprint intensity of lignin and PVA and the respective intensity ratio. The C1s high-resolution regions were curve fitted using Kratos software, Shirley backgrounds, and a fit with four symmetric Gaussian components corresponding to carbon atoms with 0, 1, 2, or 3 bonds to oxygen neighbors.[26] For the evaluation of surface lignin concentrations, the S2p, Na1s, and C−C component of the C1s high resolution signals were employed.

Local Thermal Analysis. Sub-100 nm spatial resolution local thermal analysis (TA) was performed using a nano-TA (Anasys Instruments, Santa Barbara, CA, USA). The nano-TA consists of an atomic force microscope (AFM) equipped with a ThermaLever self-heating cantilever. Temperature calibration of the ThermaLever cantilever was carried out following manufacturers protocols using melting point standards of poly(caprolactone), poly(ethylene), and poly(ethyleneterepthalate). Specimens for local thermal analysis consisted of freeze fractured samples that were glued and positioned vertically on a silicon wafer substrate using a solid lateral support, a small piece of a silicon wafer. The probe areas were cross sections of lignin/PVA 20:80 and 75:25 solvent cast films. In local thermal analysis, first the ThermaLever cantilever is used to make a high resolution contact mode AFM image. Using the AFM image, the cantilever is placed on the specimen surface within a chosen region of interest. The tip of the cantilever is then heated at a rate of 20 °C/s. During heating, the vertical deflection of the probe is monitored. Initially, an upward deflection caused by thermal expansion of the material beneath the tip is typically observed. However, when the material crosses a thermal transition, such as melting temperature, the material softens and the tip penetrates the surface resulting in a downward deflection. This downward deflection is interpreted as a material thermal transition. Using the sub-100 nm spatial resolution of the nano-TA, individual phase separated components of the lignin/PVA composites can be probed. Thermal measurements were

conducted on various locations on the specimen, and for each position, data was acquired following multiple runs. Imaging of the probed area was acquired around the indentation mark, which helped to identify the exact location of the tip−surface contact. Assessed thermal transitions were used to help identify the composition of the different phase separated components.

RESULTS AND DISCUSSION

Aqueous lignin/PVA solutions with and without CNCs were electrospun into defect-free fibers to produce randomly oriented fiber mats. We recently reported additional information about the electrospinnability of aqueous lignin/PVA/CNC solutions.[23] The fibers' radii (Table 1) increased with lignin concentration; the average radii were 89 ± 2 and 148 ± 4 nm for 20:80 and 75:25 lignin/PVA systems, respectively. With the addition of 5 wt % CNCs, the fiber radii decreased for both the 20:80 and 75:25 lignin/PVA systems. However, for CNC loadings of 15 wt %, the fiber radii increased to 104 ± 5 and 194 ± 7 nm for the 20:80/15% and 75:25/15% lignin/PVA/CNC fibers, respectively. The typical morphology and size histograms of 20:80 ligin/PVA and 20:80/15% lignin/PVA/CNC fibers are shown in Figure 1.

Figure 2 shows a field emission in-lens scanning electron microscopy (FEI-SEM) micrograph of a cross-section of an

Table 1. Radius of Electrospun Fibers and Water Contact Angle of Electrospun Fiber Mats of Different Composition, without or with CNC Loaded (Lignin/PVA and lignin/PVA/%CNC, respectively)[a]

composition		water contact angle, degrees	fiber radius, nm
Lig:PVA	0:100	50 ± 3	99 ± 8
	20:80	48 ± 0	89 ± 2
	50:50	43 ± 3	116 ± 7
	75:25	21 ± 1	148 ± 4
Lig:PVA/% CNC	20:80/0%	48 ± 0	89 ± 2
	20:80/5%	49 ± 2	68 ± 3
	20:80/10%	46 ± 1	117 ± 4
	20:80/15%	47 ± 1	104 ± 5
	75:25/0%	21 ± 1	148 ± 4
	75:25/5%	(0)	113 ± 5
	75:25/15%	(0)	194 ± 7

[a]All fibers were defect-free and without indication of beading.

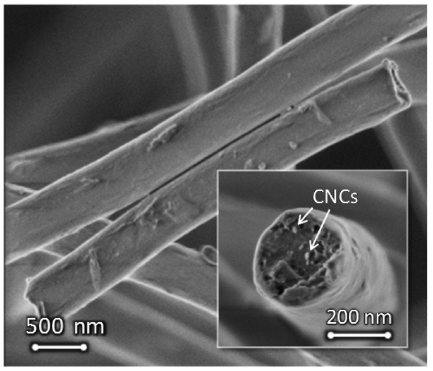

Figure 2. Field emission in-lens scanning electron microscopy (FEI-SEM) image for 75:25/15% lignin/PVA/CNC electrospun fibers. The inset shows a cross-section of the fiber prepared by the freeze fracture method. The bright features originate from the higher electron density of CNCs which allows their identification. No metal-coating was used for imaging.

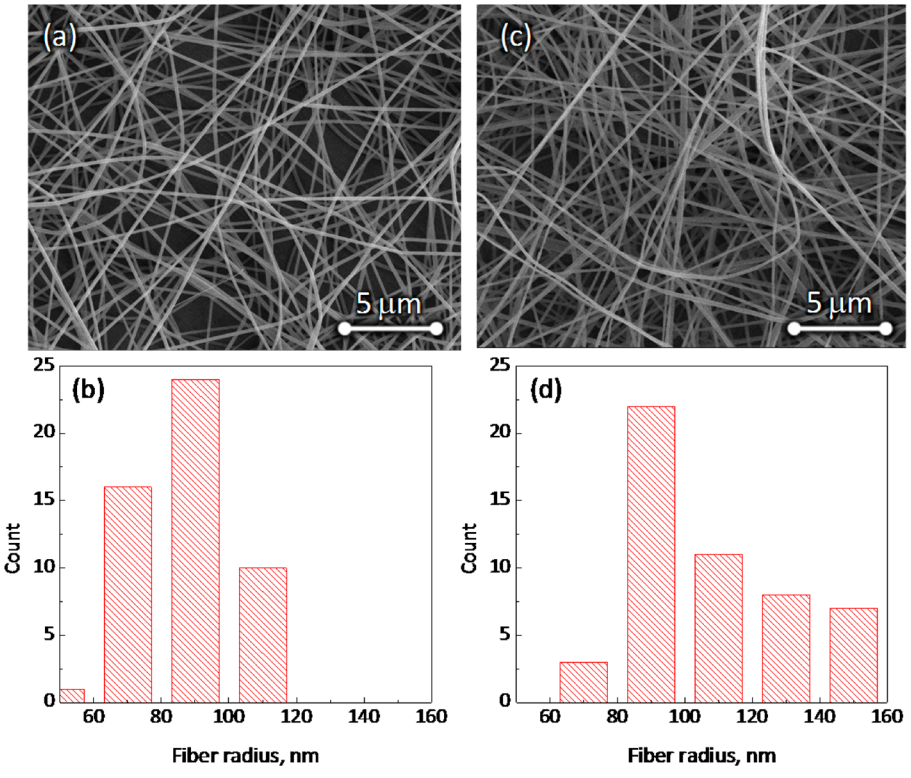

Figure 1. Field emission scanning electron microscope (FE-SEM) micrograph of electrospun fibers (top) and radius distribution (bottom) of 20:80 lignin/PVA fibers (a and b, respectively) and 20:80/15% lignin/PVA/CNC fibers (c and d, respectively).

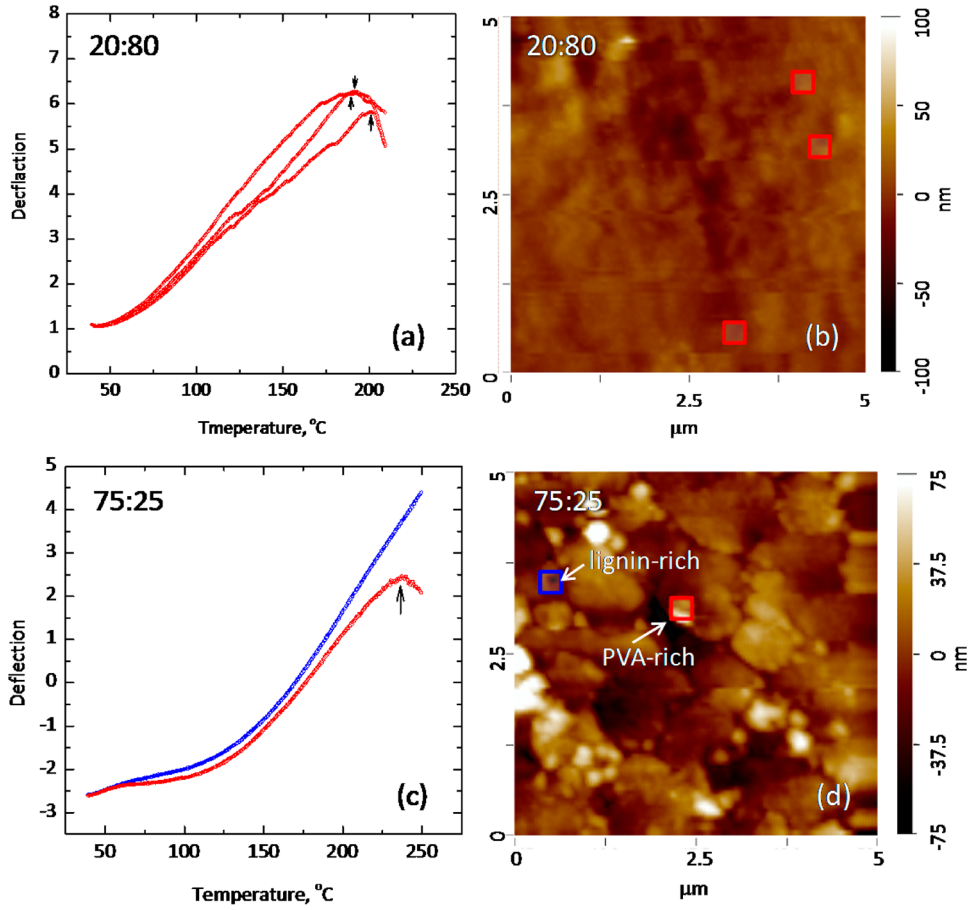

Figure 3. Local thermal analysis on cross sections of 20:80 (top) and 75:25 (bottom) lignin/PVA solvent cast films; 5 × 5 μm^2 AFM contact-mode topography images (b and d) and probe deflection profiles (a and c) are shown. The lignin-rich domains (blue curve in deflection plot, c) and PVA-rich phases (red curves) are indicated. The blue and red squares added on the AFM images represent the location of the thermal probe indentation, indicating lignin-rich and PVA-rich components, respectively.

electrospun 75:25/15% lignin/PVA/CNC fiber. Bright features in the interior of the fibers are identified as CNC nanoparticles embedded in the fibers. The detailed features in the cross sections are ascribed to the fracture of the sample, and therefore, one cannot rely on such image for any discussion on phase separation, which is better addressed in the next section.

Local Thermal Analysis. AFM-based thermal analysis combines the high spatial resolution imaging capabilities of atomic force microscopy with the ability to unveil the thermal behavior of materials with sub-100 nm spatial resolution. Because of difficulties associated with testing individual fibers, experiments were performed on reference 20:80 and 75:25 lignin/PVA solvent cast films. Figure 3 includes AFM images of film cross sections. The AFM images show phase separation in the 75:25 lignin/PVA film (Figure 3d), but no phase separation is observed in the lignin/PVA 20:80 film (Figure 3b). Three locations on the cross sections of 20:80 lignin/PVA films were randomly chosen for local thermal analysis. A clear downward probe deflection in each position is observed in the range of 191−201 °C (average 195 °C) (Figure 3a), which likely corresponds to the 200 °C melting temperature of PVA reported for Mowiol 20-98.[28] In our previous report, using differential scanning calorimetry, we found the melting temperature of 20:80 lignin/PVA electrospun fiber mats to be 220 °C.[23] The higher melting temperature observed in the electrospun fiber mats could be caused by surface effects or differences in PVA structure resulting from the higher solidification rates and smaller domains in the electrospun fibers. The AFM image in the 75:25 lignin/PVA system shows phase-separated domains with characteristic sizes on the order of 500−1000 nm (Figure 3d). The AFM-thermal probe allows the identification of two distinct phases. In the continuous, outer phase, no thermal transition is observed. However, in the round, discontinuous phase a thermal transition at 238 °C is measured (Figure 3c,d). Using thermogravimetric analysis on 75:25 lignin/PVA electrospun fiber mats, we previously observed a degradation peak at about 233 °C that corresponds to the dehydration of PVA. It is possible that the thermal transition of the discontinuous phase corresponds to this PVA degradation peak. The lack of PVA melting temperature and presence of PVA degradation peak suggests that the discontinuous phase is a lignin/PVA composite in which the molecular interactions between lignin and PVA prevent the formation of crystalline PVA regions. The lack of thermal transition in the continuous phase suggests that it is primarily lignin, which has no melting temperature and a thermal degradation peak at around 308 °C.[23]

Surface Composition and Water Contact Angle. Pure lignin solutions did not produce fibers upon electrospinning, but the water contact angle (WCA) for such system can be expected to be similar to that measured on a thin film prepared by spin coating (5 wt % lignin aqueous solution), 10 ± 1°. This low WCA supports the hydrophilic character of the lignin employed here.[29] The WCA of neat PVA electrospun fibers was

50 ± 3°. The change in WCA of electrospun fiber mats as a function of wt % lignin in the solid fiber is shown in Figure 4a.

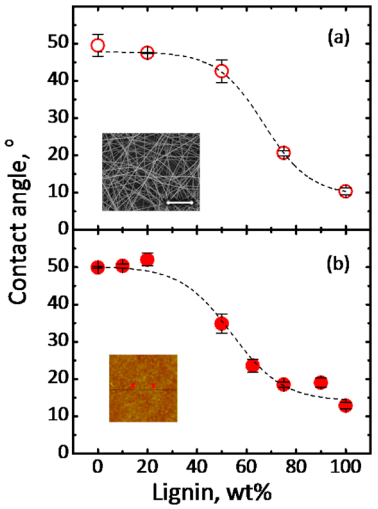

Figure 4. Water contact angles of bicomponent lignin/PVA electrospun fiber mats (a) and spin coated films (b) as a function of lignin wt % based on total solids. The error bars indicate the standard deviation calculated from three different samples. Typical surface morphologies from SEM analyses of electrospun fiber mats (500 nm scale bar) and from an AFM scan (1 × 1 μm^2) of spin coated films are added as insets in (a) and (b), respectively.

The WCA of the lignin/PVA fiber systems roughly remained unchanged as the amount of lignin was increased from 0 to 40 wt %. Above this 40 wt % threshold value, a substantial WCA reduction is observed. The addition of CNCs to 20:80 lignin/PVA systems was observed not to produce changes in the WCA (Table 1); however, WCA decreased rapidly, close to 0°, in the 75:25 lignin/PVA systems with the addition of CNCs.

The WCA results can be used to assess the distribution of PVA and lignin on the surface of the fibers and gain insights into the influence of CNC addition. In Figure 4a, the near constant contact angle below 40 wt % lignin suggests that the fiber surfaces are dominated by PVA for these compositions. To better judge the influence of such effects, we examined further the WCA for spin coated lignin/PVA films (Figure 4b). All lignin/PVA composite films were continuous and smooth with an average root-mean-square (RMS) roughness of 0.6 nm. Noting that the WCA depends not only on the chemical composition (surface energy) but also on the surface roughness and morphology, it is interesting to observe that the WCA values of the spin coated films were similar to those obtained from the electrospun fiber mats (Figure 4a,b). This observation can be taken as an indication that electrospinning and spin coating produce bicomponent materials with similar surface chemical composition and that their differences in surface roughness/morphology did not affect the WCA. This unexpected observation was confirmed after repeated measurements. With the addition of CNCs, no differences in WCA were observed in 20:80 lignin/PVA fiber mats (Table 1). This suggests that the CNCs did not influence the PVA-rich surface of these fibers. However, WCA decreased to 0° with the addition of CNCs to the 75:25 lignin/PVA system, suggesting strong interactions between the lignin-rich domains of these fibers and the CNCs.

The surface chemical composition of 75:25, 50:50, and 20:80 lignin/PVA electrospun fibers and pure PVA and lignin spin-coated films were determined using XPS (Figure 5). From the C1s high resolution spectra (Figure 5b), it is observed that as the amount of PVA increases the relative intensity of the C−O contribution (at ca. 286.6 eV binding energy) also increases.

Both Na and S signals originate only from lignin and can be used to identify and quantify surface lignin (Figure 5a,c, respectively); the C−C signal, typically used in quantitative determinations in lignocelluloses, is also available. Calculations based on the S2p signal are reported here in our quantitative

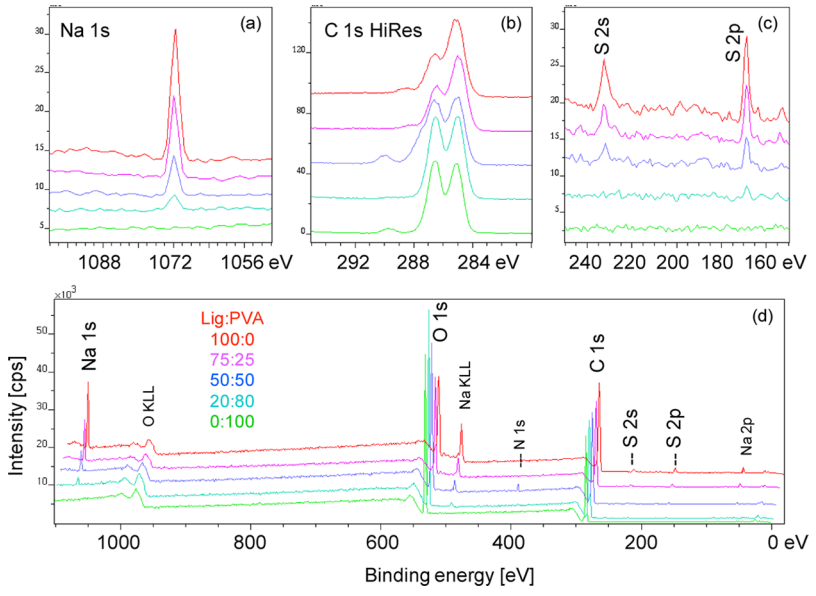

Figure 5. XPS spectra of lignin/PVA electrospun fibers (75:25, 50:50, and 20:80 lignin/PVA compositions, indicated by violet, blue, and light blue, respectively). Included are also reference spectra for spin coated films of pure lignin (100:0, red) or pure PVA (0:100, bright green). From top to bottom, the spectra are lignin/PVA 100:0, 75:25, 50:50, 20:80, and 0:100. The survey scans shown in (d) include the contributions from the main atomic surface components, which are analyzed in high resolution for Na 1s (a), C 1s (b), and S2s and S2p (c).

analyses, but we note that the compositions calculated from Na 2p or C−C component of the C1s signals are in close agreement, within a ±10% deviation. The lignin surface concentration in the electrospun fiber (calculated from the S2p signal intensity) plotted against the lignin wt % is shown in Figure 6. From this figure, it can be concluded that the surface

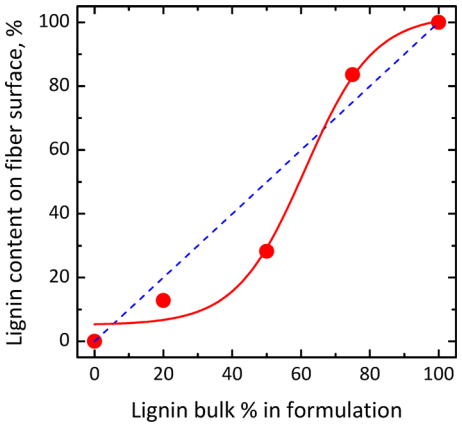

Figure 6. Lignin surface concentration of bicomponent (lignin/PVA) electrospun fibers as a function of the total lignin wt % in the fiber. The lignin concentrations were calculated from the S 2p XPS signal intensity. Lines are added as guides to the eye.

of the fibers is depleted in lignin when the lignin bulk composition is under ca. 50 wt %, which is in close agreement with the WCA analysis (Figure 4a). It is noted that the amount of lignin on the surface is significantly increased at bulk concentrations above the threshold concentration of ca. 50% lignin. These results support the hypothesis that a thin layer of PVA is formed at the air−solid interface during the formation of fibers when the dominant component in the precursor polymer mixture is PVA.

The nonlinear relationship between the surface and the bulk composition obtained from XPS (Figure 6) and WCA (Figure 4) analyses reveal the existence of interesting phase separation phenomena in electrospun fibers. During the extremely rapid solvent evaporation and solidification during electrospinning, it is expected that polymer structure is quenched into a nonequilibrium thermodynamic state and the polymer chains are locked into highly strained states near the surface. However, our XPS (Figure 6) and WCA (Figure 4) results show that surface composition is not directly proportional to fiber composition. There is a threshold value around 40−50 wt % lignin above which lignin dominates the surface. The nonlinear behavior suggests that, despite the extremely fast quenching during electrospinning, some phase separation processes might still be occurring.

Further insights can be gained looking at the structures of solvent-cast films which are expected to be closer to thermodynamic equilibrium because of their "slow" solidification. Between lignin and PVA, PVA has lower surface energy and is therefore more likely to enrich the surface at an air/solid interface during solidification. In 20:80 lignin/PVA solvent cast films, no phase separation could be observed (Figure 3b) and using local thermal analysis we found evidence of crystalline PVA domains throughout the continuous phase. In contrast, in the 75:25 lignin/PVA solvent cast film, we observed phase separation (Figures 3d and 7) with the discontinuous phase having PVA and the continuous phase, which would be expected to also be on the surface, to be lignin-rich. So despite PVA's lower surface energy, for the 75:25 lignin/PVA systems, it is possible that a lignin-rich surface is more thermodynamically favorable. Figure 8 shows schematically the proposed component distribution in lignin/PVA

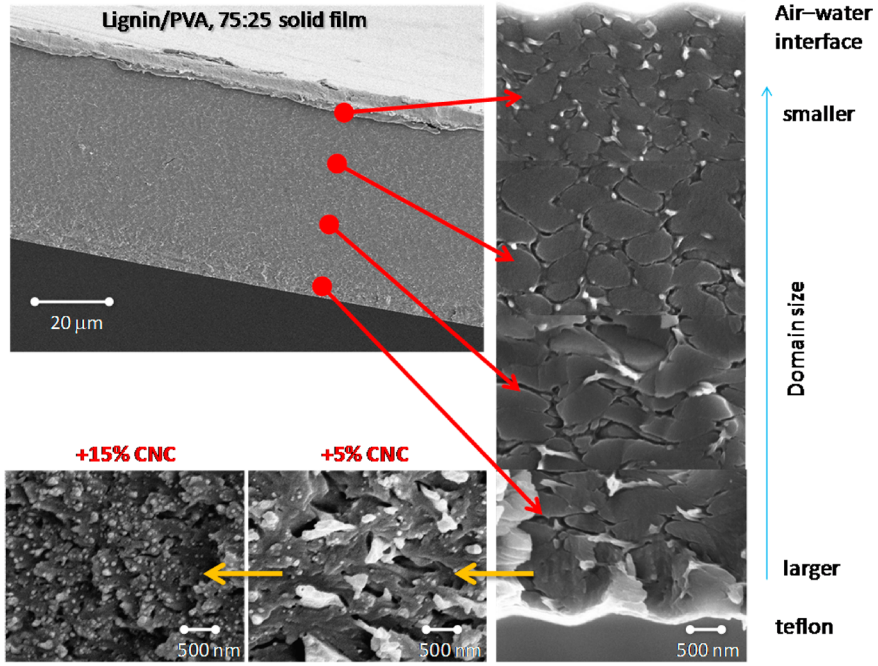

Figure 7. SEM images of cross sections of lignin/PVA (75:25) films. The two interfaces indicated correspond to the air/film interface and film/Teflon support. The size of the domains is reduced as they are closer to the air/film interface. The addition of CNC to the aqueous dispersion used as precursor of the films is observed to reduce the characteristic size of the phase-separated domains (see images in bottom panels with cross sections of films loaded with 5 and 15% CNCs).

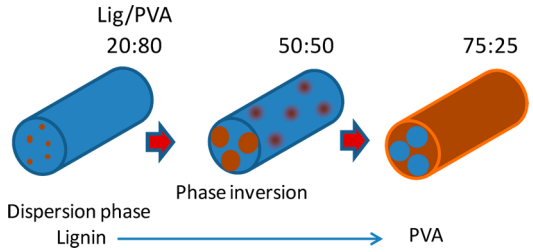

Figure 8. Schematic representation of proposed surface composition of composite electrospun lignin/PVA fibers. The exact distributions, size, and number of domains are unknown.

electrospun fibers. For lignin contents under 50%, lignin is the dispersed phase within a continuous PVA matrix, but at higher concentrations, discontinuous PVA/lignin phases form within a continuous lignin-rich phase.

One question that emerges is to what extent does the addition of CNCs influence component distribution in the fibers. WCA of 75:25 lignin/PVA electrospun fiber mats decreased with the addition of 5 and 15 wt % CNCs from 21 ± 1° to 0°. However, for 20:80 lignin/PVA electrospun fiber mats, the WCA remained unchanged with 48 ± 0, 49 ± 2, 46 ± 1, and 47 ± 1 for CNC 0, 5, 10, and 15 wt %, respectively (Table 1). We also note that in the case of 75:25 lignin/PVA systems the WCA was lower than that compared to pure lignin spin-coated films (Figure 4b) after CNCs were added (Table 1). These results indicate that CNCs affect the surface polymer distribution of the 75:25 lignin/PVA electrospun fibers, possibly because the CNCs are more prevalent in the lignin phase which dominates the surfaces of these fibers. We also point out the observation that in the 75:25 lignin/PVA systems the addition of CNCs reduces the characteristic domain size in solvent cast films, i.e., improves the compatibility or mixing of the lignin and PVA polymers (Figure 7). These observations in WCA and morphology highlight the strong interaction that exists between CNCs and lignin, which is the principal component in 75:25 lignin/PVA systems.

CONCLUSIONS

The surface structure and interfacial properties of lignin/PVA/CNC electrospun fibers were studied by WCA, XPS, and local thermal analyses. The results indicate that the surface composition of the electrospun fibers is not directly proportional to the bulk composition. Below a threshold of about 50 wt % lignin, PVA dominates the electrospun fiber surfaces, and above the threshold, lignin dominates. In 75:25 lignin/PVA solvent-cast films, phase separated domains are observed. Using local thermal analysis, the continuous phase is determined to be lignin-rich and the discontinuous phase has a PVA/lignin material with suppressed PVA crystallinity. The sizes of the phase-separated domains are reduced by addition of CNCs to the system. Also, the addition of CNCs affected the 75:25 lignin/PVA electrospun fiber surfaces but not the 20:80 lignin/PVA electrospun fiber surfaces, suggesting CNCs are more closely associated with lignin.

ASSOCIATED CONTENT

Supporting Information

AFM images of cellulose nanocrystals and spin coated films used in this study and XPS analyses of bicomponent fiber mats and lignin or PVA films. This material is available free of charge via the Internet at http://pubs.acs.org.

AUTHOR INFORMATION

Corresponding Author

*E-mail: ojrojas@ncsu.edu (O.J.R.); ago@fe.bunri-u.ac.jp (M.A.). Tel: +1-919-513 7494. Fax: +1-919-515 6302.

Notes

The authors declare no competing financial interest.

ACKNOWLEDGMENTS

The authors acknowledge financial support of Asahikasei Fibers Corporation, Japan. Tokushima Bunri University is gratefully acknowledged for funding M.A. during her international exchange program with NC State University (O.J.R.). Partial funding support from US Department of Agriculture under grant number 2011-10006-30377 is highly appreciated.

REFERENCES

(1) Li, W.-J.; Laurencin, C. T.; Caterson, E. J.; Tuan, R. S.; Ko, F. K. *J. Biomed. Mater. Res.* **2002**, *60*, 613−621.
(2) Huang, Z.-M.; Zhang, Y. Z.; Kotaki, M.; Ramakrishna, S. *Compos. Sci. Technol.* **2003**, *63*, 2223−2253.
(3) Darrell, H. R.; Iksoo, C. *Nanotechnology* **1996**, *7*, 216−223.
(4) Yoon, K.; Kim, K.; Wang, X.; Fang, D.; Hsiao, B. S.; Chu, B. *Polymer* **2006**, *47*, 2434−2441.
(5) Ding, B.; Kim, J.; Miyazaki, Y.; Shiratori, S. *Sens. Actuators, B* **2004**, *101*, 373−380.
(6) Kim, K.; Yu, M.; Zong, X.; Chiu, J.; Fang, D.; Seo, Y.-S.; Hsiao, B. S.; Chu, B.; Hadjiargyrou, M. *Biomaterials* **2003**, *24*, 4977−4985.
(7) Li, D.; Xia, Y. *Adv. Mater.* **2004**, *16*, 1151−1170.
(8) Zussman, E.; Chen, X.; Ding, W.; Calabri, L.; Dikin, D. A.; Quintana, J. P.; Ruoff, R. S. *Carbon* **2005**, *43*, 2175−2185.
(9) Teo, W. E.; Ramakrishna, S. *Nanotechnology* **2006**, *17*, R89−R106.
(10) Greiner, A.; Wendorff, J. H. *Angew. Chem., Int. Ed.* **2007**, *46*, 5670−5703.
(11) Aden, A.; Ruth, M.; Ibsen, K.; Jechura, J.; Neeves, K.; Sheehan, J.; Wallace, B.; Montague, L.; Slayton, A.; Lukas, J. *Lignocellulosic Biomass to Ethanol Process Design and Economics Utilizing Co-Current Dilute Acid Prehydrolysis and Enzymatic Hydrolysis for Corn Stover*; National Renewable Energy Laboratory: Golden, CO, 2002.
(12) Kubo, S.; Kadla, J. F. *J. Polym. Environ.* **2005**, *13*, 97−105.
(13) Kadla, J. F.; Kubo, S.; Venditti, R. A.; Gilbert, R. D.; Compere, A. L.; Griffith, W. *Carbon* **2002**, *40*, 2913−2920.
(14) Hatakeyama, H.; Hirose, S.; Hatakeyama, T.; Nakamura, K.; Kobashigawa, K.; Morohoshi, N. *J. Macromol. Sci., Part A* **1995**, *32*, 743−750.
(15) Saraf, V. P.; Glasser, W. G. *J. Appl. Polym. Sci.* **1984**, *29*, 1831−1841.
(16) Cook, P. M.; Sellers, T. Organosolv Lignin-Modified Phenolic Resins. In *Lignin*; American Chemical Society: Washington, DC, 1989; Vol. *397*, pp 324−333.
(17) Sarkar, S.; Adhikari, B. *J. Adhes. Sci. Technol.* **2000**, *14*, 1179−1193.
(18) Glasser, W. G.; Leitheiser, R. H. *Polym. Bull.* **1984**, *12*, 1−5.
(19) Suhas; Carrott, P. J. M.; Ribeiro Carrott, M. M. L. *Bioresour. Technol.* **2007**, *98*, 2301−2312.
(20) Gupta, V. K.; Suhas. *J. Environ. Manage.* **2009**, *90*, 2313−2342.
(21) Guo, X.; Zhang, S.; Shan, X.-Q. *J. Hazard. Mater.* **2008**, *151*, 134−142.
(22) Khan, M. A.; Ashraf, S. M.; Malhotra, V. P. *Int. J. Adhes. Adhes.* **2004**, *24*, 485−493.
(23) Ago, M.; Okajima, K.; Jakes, J. E.; Park, S.; Rojas, O. J. *Biomacromolecules* **2012**, *13*, 918−926.
(24) Ebeling, T.; Paillet, M.; Borsali, R.; Diat, O.; Dufresne, A.; Cavaillé, J. Y.; Chanzy, H. *Langmuir* **1999**, *15*, 6123−6126.
(25) Elazzouzi-Hafraoui, S.; Nishiyama, Y.; Putaux, J.-L.; Heux, L.; Dubreuil, F.; Rochas, C. *Biomacromolecules* **2007**, *9*, 57−65.

(26) Johansson, L.-S.; Campbell, J. M. *Surf. Interface Anal.* **2004**, *36*, 1018−1022.
(27) Beamson, G.; Briggs, D. *High resolution XPS of organic polymers: the Scienta ESCA300 database*; Wiley: Chichester (England) and New York (USA), 1992.
(28) http://www.kuraray-am.com/pvoh-pvb/downloads/Mowiol_brochure_en_KSE.pdf.
(29) Notley, S. M.; Norgren, M. *Langmuir* **2010**, *26*, 5484−5490.